

# Altair: Automatic Image Analyzer to Assess Retinal Vessel Caliber

Gabino Verde, Luis García-Ortiz, Sara Rodríguez,  
José I. Recio-Rodríguez, Juan F. De Paz, Manuel A. Gómez-Marcos,  
Miguel A. Merchán, and Juan M. Corchado

**Abstract.** The scope of this work is to develop a technological platform specialized in assessing retinal vessel caliber and describing the relationship of the results obtained to cardiovascular risk. Population studies conducted have found retinal vessel caliber to be related to the risk of hypertension, left ventricular hypertrophy, metabolic syndrome, stroke, and coronary artery disease. The vascular system in the human retina has a unique property: it is easily observed in its natural living state in the human retina by the use of a retinal camera. Retinal circulation is an area of active research by numerous groups, and there is general experimental agreement on the analysis of the patterns of the retinal blood vessels in the normal human retina. The development of automated tools designed to improve performance and decrease interobserver variability, therefore, appears necessary.

## 1 Introduction and Background

Image processing, analysis and computer vision techniques are increasing in prominence in all fields of medical science, and are especially pertinent to modern ophthalmology, which is heavily dependent on visually oriented signs. Automatic detection of parameters from retinal images is an important problem since are associated with the risk of hypertension, left ventricular hypertrophy, metabolic syndrome, stroke, and coronary artery disease [14] [15].

The vascular system in the human retina has a unique property: it is easily observed in its natural living state in the human retina by the use of a retinal camera.

---

Gabino Verde · Sara Rodríguez · Juan F. De Paz · Juan M. Corchado  
Computers and Automation Department, University of Salamanca, Salamanca, Spain

Luis García-Ortiz · José I. Recio-Rodríguez · Manuel A. Gómez-Marcos ·  
Miguel A. Merchán  
Primary care Research unit La Alamedilla. Sacyl. IBSAL. Salamanca, Spain  
e-mail: {gaby, lgarciao, srg, donrecio, fcofds, magomez}@usal.es,  
merchan, corchado@usal.es

The retina is the only human location where blood vessels can be directly visualized non-invasively. The identification of landmark features such as the optic disc, fovea and the retinal vessels as reference co-ordinates is a prerequisite to systems being able to achieve more complex tasks that identify pathological entities. Reliable techniques exist for identifying these structures in retinal photographs. The most studied areas in this field can be classified into three groups [10]:

1. The *location of the optic disc*, which is important in retinal image analysis for vessel tracking, as a reference length for measuring distances in retinal images, and for identifying changes within the optic disc region due to disease. Techniques such as analysis of intensity pixels with a high grey-scale value [8] [3] or principal component analysis (PCA) [9] are used for locating the disk. Other authors [7] use the Hough transform (a general technique for identifying the locations and orientations of certain types of shapes within a digital image [7]) to locate the optic disc. A “fuzzy convergence” algorithm is another technique used for this goal [4].

2. The *detection of the fovea*, usually chosen as the position of maximum correlation between a model template and the intensity image [9].

3. The segmentation of the vasculature from retinal images, that is, the representation of the blood vessels and their connections by segments or similar structures. There are a lot of techniques to do this, the most significant of which are: (i) matched filters, which typically have a Gaussian or a Gaussian derivative profile; (ii) vessel tracking, whereby vessel centre locations are automatically sought over each cross-section of a vessel along the vessels longitudinal axis, having been given a starting and end point [13]; (iii) neural networks, which employ mathematical “weights” to decide the probability of input data belonging to a particular output [1]; (iv) morphological processing, which uses characteristics of the vasculature shape that are known a priori, such as being piecewise linear and connected [4].

An understanding of the design principles of the human vascular system may have applications in the synthetic design of vascular systems in tissue and organ engineering, i.e., bioartificial organs for both liver and kidney. In current scientific literature one can find a lot of research devoted to automating the analysis of retinal images [12] [2] [4]. In this paper, after several years of studies and tests, we propose a novel platform image processing to study the structural properties of vessels, arteries and veins that are observed with a red-free fundus camera in the normal human eye, and the fractal analysis of the branching trees of the vascular system. The platform, called Altair “Automatic image analyzer to assess retinal vessel caliber”, employs analytical methods and AI (Artificial Intelligence) algorithms to detect retinal parameters of interest. The sequence of algorithms represents a new methodology to determine the properties of retinal veins and arteries. The platform does not require user initialization, it is robust to the changes in the appearance of retinal fundus images typically encountered in clinical environments, and is intended as a unified tool to link all the methods needed to automate all processes of measurement on the retinas. The platform uses the latest computer techniques both statistical and medical. The next section introduces the Altair platform. Section 3 presents the most important characteristics of the platform, showing some of the relevant techniques and results. Finally, some conclusions are presented in section 4.

## 2 Platform Overview

Altair facilitates the study of structural properties of vessels, arteries and veins that are observed with a red-free fundus camera in the normal human eye, and the fractal analysis of the branching trees of the vascular system. Figure 1 shows an example of images taken directly from the fundus. The retinal vessels appear in a different color, with the optic disc and fovea. There are many patterns in nature that show branching, such as the retinal vessel, and those with open branching structures and different lengths. These objects can be described by fractal geometry. Different analytical methods and AI algorithms are used to determine the scaling properties of real objects, yielding different measures of the fractal dimension, length and area of retinal veins and arteries.

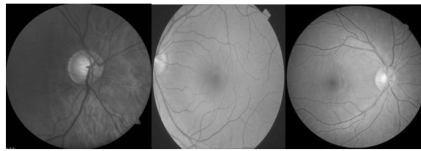


**Fig. 1** Retinograph usually takes three images of each eye: a) Centered papilla. b) With the disc on one side. c) With the macula and disc each to one side of center

The main objective is to relate the level of cardiovascular risk in patients to everything that can be observed in the retinas. In this work we are interested in obtaining as much information as possible from the images obtained, and have focused on the following:

- Index Artery / Vein: represents a relationship between the thickness of arteries and veins.
- Branching: branching structures include fractal analysis of the branching trees of the vascular system. More branches tend to appear in subjects with cardiovascular diseases, especially around the papilla. Branching index refers to the number of times that an artery branches, while branching pattern refers to the way in which arteries branch. Actually the manner in which branching occurs is practically a fingerprint in that each person has a different shape, however in many samples retinas it is possible to observe certain normal patterns. In that case the relationship of these patterns with the diseases could be studied.
- Area occupied by the veins and arteries.
- Distribution of the capillary: according to the blood distribution, the color distribution of the capillaries varies.

Moreover, our intention is to incorporate expert knowledge taken from the measurements found in the retinal circulation which specify normal values of various retinal structures in healthy subjects, and to apply this information to the study of patients suffering from a number of diseases. Based on the values for area, length, position and patterns of the branching trees of the vascular system in healthy pa-

tients, we expect to determine ranges of normalcy within the population for their subsequent application to subjects affected by various diseases. The next section explains the main components of the platform. The original image passes through each one of the modules (preprocessing, detection, segmentation and extraction of knowledge), which use different techniques and algorithms to obtain the desired image information. This sequence of steps is a methodology that is explained in the following section, also showing examples of the results obtained.

### 3 Methodology and Results

The methodology used to obtain the functionality of the platform may be divided into two phases. Firstly, a phase called "digitization of the retina", in which the different parts of the eye image are identified. Here a data structure is created, which makes it possible to represent and process the retina without requiring the original image. This phase includes modules of preprocessing, detection and segmentation. Secondly, a phase of "measurements" in which we work with retinas that have been previously identified. This phase includes extraction of knowledge and manual correction, or expert knowledge, if necessary.

This paper focuses on the first phase, which is in charge of creating and identifying all the elements of interest of the retina. To carry out these phases, the following steps are necessary.

#### *Preprocessing*

The preprocessing or filtering module reduces noise, improves contrast, sharpens edges or corrects blurriness. Some of these actions can be carried out at the hardware level, which is to say with the features included with the camera. During the testing, retinography was performed using a Topcon TRC NW 200 nonmydriatic retinal camera (Topcon Europe B.C., Capelle a/d IJssel, The Netherlands), obtaining nasal and temporal images centered on the disk (Figure 1). The nasal image with the centered disk is loaded into the platform software through the preprocessing module.

#### *Detection limits*

This module is in charge of locating the disk and identifying the center and edges of the retina. The goal here is to construct a data structure that identifies each part of the retina based on the matrices of colors representing the images obtained (Figure 1). In this step, image processing techniques were used to detect intensity based on the boundaries of the structures [4] [2]. The identification of the papilla is important since it serves as the starting point for the detection and identification of the different blood vessels. This phase identifies the boundaries and the retinal papilla from a RGB image of the retina. The following values are returned: Cr is the center of the retina, which identifies the vector with coordinates  $x$ ,  $y$  of the center of the retina. Cp is the center of the disc, which identifies the vector with the coordinates  $x$ ,  $y$

of the center of the papilla.  $R_r$  is the radius of the retina.  $R_p$  is the radius of the papilla. As an example, a sequence of output values in this phase is shown in the following table and figure:

| $C_r$               | $C_p$  | $R_r$  | $R_p$                                |
|---------------------|--|--------|--------------------------------------|
| 1012,44 ;<br>774,13 | 1035,98 ; 734,11<br>1104,87 ; 562,52<br>915,38 ; 736,77<br>900,27 ; 658,74 | 692,68 | 111,76<br>108,92<br>122,15<br>101,95 |

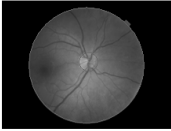


**Fig. 2** Identification result in the detection phase. Table 1. equence of output values in detection modules (pixel).

In order to identify the limits, and in particular to identify the circumferences, it became necessary to carry out a process of image segmentation. Segmentation is the process that divides an image into regions or objects whose pixels have similar attributes. Each segmented region typically has a physical significance within the image. It is one of the most important processes in an automated vision system because it makes it possible to extract the objects from the image for subsequent description and recognition. Segmentation techniques can be grouped into three main groups: techniques based on the detection of edges or borders [7], thresholding techniques [8], and techniques based on clustering of pixels [3]. After analyzing the possibilities, we chose one of the techniques from the first group that provided the best results, which in this case uses an optimization of the Hough transform [7]. This technique is very robust against noise and the existence of gaps in the border of the object. It is used to detect different shapes in digital images. When applying the Hough transform to an image, it is first necessary to obtain a binary image of the pixels that form part of the limits of the object (applying edge detection). The aim of the Hough transform is to find aligned points that may exist in the image to form a desired shape. For example, to identify line points that satisfy the equation of the line:  $\rho = x \bullet \cos\theta + \text{sen}\theta$ , in polar coordinate. In our case, we looked for points that verify the equation of the circle: (i) in polar coordinate system:  $r^2 - 2sr \bullet \cos(\theta - \alpha) + s^2 = c^2$ , where  $(s, \alpha)$  is the center and  $c$  the radius; (ii) in Cartesian coordinate system:  $(x - a)^2 + (y - b)^2 = r^2$ , where  $(a, b)$  is the center and  $r$  the radius. The algorithm is not computationally heavy, as it does not check all radii, or all possible centers, only the candidate values. The candidate centers are those defined in a near portion of the retina, and the radius is approximately one sixth the radius of the retina. To measure the approximate diameter of the retina, the algorithm calculates the average color of the image column: diameter of the retina is the length that has a non-zero value (black).

Identifying the papilla (Figure 3) is a necessary step because it provides a starting point for other stages of segmentation and serves as a reference point for some typical measurements. Typically the correct result is the circumference of the higher value in the accumulator (over 70% of cases). In almost 100% of the cases, the cor-

```

load image
detect edges
for each candidate point (a, b) in the image
  for each candidate radius r
    calculate the points (x, y) which are at an edge and
    y is in the circumference of center (a, b) and radius r and
    introduce them into the accumulator
find the pairs (center, radius) whose values are the highest in the accumulator

```

Fig. 3 Pseudocode of the identification algorithm of the papilla

rect identification can be found among the 3 greatest values found by the accumulator.

**Segmentation of the vasculature from retinal images**

The ultimate goal in this module is to identify each blood vessel as a series of points that define the path of the vessel. Each of these points will be assigned a certain thickness. Moreover, it will be necessary to distinguish whether a particular blood vessel is a vein or an artery. AI algorithms responsible for identifying veins and arteries must perform a series of sweeps in search of "key points". Algorithms based on matched filters [6], vessel tracking [12] and PCA [9], among others, are used for obtaining the proximity points between objects (veins, arteries, capillaries), the structures retinal structures or assemblies, branching patterns, etc. These algorithms work with transformations of the original image of the retina obtained from the previous step. Three steps are necessary within this module: (i) identification of vessels; (ii) definition of the structure of vessel; (iii) cataloging of veins and arteries.

*Identification of vessels.* In this step the blood vessels are identified in the image by thresholding techniques. Their purpose is to remove pixels where the structuring element does not enter, in this case the blood vessels. The image on the retina is blurred to keep an image similar to the background. This image is used as a threshold so that the pixels of the original image will be treated as vessels if their intensity reaches 90% of the background intensity.

The image below represents the application of these techniques in a row. The blue line represents the values of the pixels in the image; the red line, the background values; and the green line the point where there is a vessel:

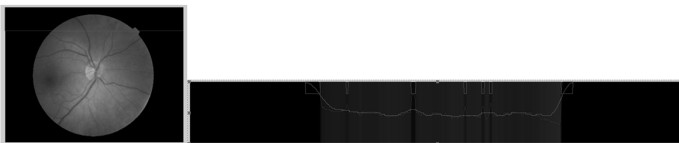


Fig. 4 Thresholding techniques for the identification of vessels

In the figure, it is possible to observe a very small vessel on the left, which comes from the artery below. In the middle there is a fat vein and to the right there are three tiny vessels. Furthermore the edge of the retina is marked as a vessel although obviously it is not. To decide where there is a vessel, the following algorithm is

applied (Figure 5a) where  $Original(x,y)$  is the pixel  $(x,y)$  of the original image and  $Background(x,y)$  is the pixel  $(x,y)$  of the background image. The result is shown in Figure 5b.

```

If (Original (x, y) <Background (x, y) * threshold)
  There is vessel at (x, y)
If not
  There is not vessel at (x, y)
Threshold ~0.9

```



**Fig. 5** a) Pseudocode of the identification algorithm of the papilla. b) Image result. (Blank pixels are the vessels).

*Structure of vessel.* This phase defines the tree forming blood vessels. Various techniques are used in conjunction with the following steps:

The following image shows the output of this phase. At the end of this stage the entire arterio-venous tree is stored in a structured way, making it possible to know not only if a vessel passes through a point or not, but through which point each vessel passes, which one is its parent, etc.

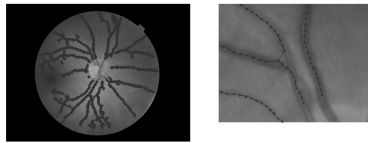


**Fig. 6** Structure of the vessels

*Cataloging of veins and arteries.* To detect whether a vessel is vein or artery, main branch is taken of the vessel. For every point  $(x,y)$  of the branch:

```

If (Original (x,y) < Background (x,y) * threshold)
  Probable vein
If not
  Not vein
Threshold ~0.7

```

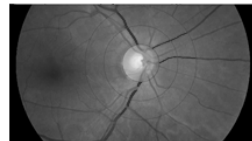


**Fig. 7** a)Pseudocode of the identification algorithm of veins. b)Arteries and veins detection.

In general, if most points of the main branch of the vessel (from at least 60%) are points classified as "probable vein", we conclude that this vessel is a vein, otherwise an artery. Currently, there are no publicly available databases that can be used to assess the performance of automatic detection algorithms on retinal images. In this

study, we assessed the performance of our platform using retinal images acquired from the Primary Care Research Unit La Alamedilla, SACYL, IBSAL, Salamanca, Spain . The images were obtained using a TopCon TRC-NW6S Non-Mydriatic Retinal Camera. Table 2 shows the testing performed using 10 retinal images. No difference was found between values in terms of age, sex, cardiovascular risk factors, or drug use. The first row of values is shown in the examples retina and previous figures in this paper. The table shows: Area veins and arteries, Diameter of veins and arteries (D), AV index (AV), Veins P (VP) = number of veins around the papilla, Veins A (VA)= number of veins that cross the corona outlined with radius=2\*Rp. Rp is the radio of the papilla, Veins B (VB)= number of veins that cross the corona outlined with radius=3\*Rp, same values for arteries. And the ratios leaving the region around the papilla and out of the disc (which could serve as a reference of bifurcations that have occurred, though not in the manner in which they branch).

| Ret | Area veins (mm <sup>2</sup> ) | Area arteries (mm <sup>2</sup> ) | R <sub>p</sub> (mm) | V <sub>p</sub> | V <sub>a</sub> | V <sub>b</sub> | A <sub>p</sub> | A <sub>a</sub> | A <sub>b</sub> | Veins Thickness (mm) | Arteries Thickness (mm) | AV Index   | Veins B/P  | Veins B/P |
|-----|-------------------------------|----------------------------------|---------------------|----------------|----------------|----------------|----------------|----------------|----------------|----------------------|-------------------------|------------|------------|-----------|
| 1   | 2.200147433                   | 1.597102803                      | 1.13693             | 5              | 6              | 8              | 7              | 9              | 12             | 0.12084217           | 0.083101875             | 0.68768956 | 1.6        | 1.7142857 |
| 2   | 2.004176495                   | 1.995543005                      | 1.04058             | 4              | 5              | 6              | 5              | 8              | 11             | 0.15342774           | 0.098325175             | 0.64085657 | 1.5        | 2.2       |
| 3   | 1.637113923                   | 1.377180899                      | 0.973135            | 5              | 6              | 6              | 4              | 6              | 10             | 0.12165151           | 0.08752424              | 0.71946776 | 1.2        | 2.5       |
| 4   | 1.698848018                   | 1.463144459                      | 1.05985             | 5              | 6              | 8              | 6              | 9              | 10             | 0.12091925           | 0.08029809              | 0.66406375 | 1.6        | 1.6666667 |
| 5   | 2.04780811                    | 1.156423484                      | 1.0357625           | 6              | 6              | 10             | 6              | 6              | 8              | 0.112816215          | 0.098999625             | 0.87753011 | 1.66666667 | 1.3333333 |
| 6   | 1.845338847                   | 1.641012918                      | 1.07912             | 5              | 5              | 7              | 7              | 8              | 11             | 0.11180454           | 0.083313845             | 0.74517408 | 1.4        | 1.5714286 |
| 7   | 1.737095306                   | 1.240139053                      | 1.0800835           | 5              | 7              | 8              | 8              | 8              | 11             | 0.12290406           | 0.07943021              | 0.64644089 | 1.6        | 1.375     |
| 8   | 1.612513118                   | 1.261882027                      | 1.0396165           | 5              | 6              | 8              | 7              | 10             | 12             | 0.12195983           | 0.08199385              | 0.6723021  | 1.6        | 1.7142857 |
| 9   | 1.566189539                   | 1.183139453                      | 0.9008725           | 6              | 7              | 8              | 6              | 7              | 7              | 0.100271445          | 0.094124251             | 0.93869511 | 1.33333333 | 1.6666667 |
| 10  | 1.609078289                   | 1.13962067                       | 0.934595            | 6              | 7              | 8              | 5              | 6              | 9              | 0.13317497           | 0.099808965             | 0.74945739 | 1.33333333 | 1.8       |

Fig. 8 Output results for 10 retinal images. Table 2.

It is possible to observe that the measurement values of veins and arteries (thickness, area) are similar between different retinas (in this case no retinal images of sick patients were introduced). Parameters like the veins in the papilla and AV index are the most fluctuating. Due to the lack of a common database and a reliable way to measure performance, it is difficult to compare our platform to those previously reported in literature. Although some authors report algorithms and methods [12] [2] [4] with similar performance to our platform, these results may not be comparable, since these methods are tested separately and were assessed using different databases. Since automation has been valid and verified our next step is to compare the values obtained with significant medical values in our database.

**Knowledge extraction**

This platform will show a high intra-observer and inter-observer reliability with the possibility of expert corrections if necessary. Results of its validity analysis must be consistent with the findings from large studies conducted with regards to both cardiovascular risk estimation and evaluation of target organ damage. The results obtained during the use of the platform will be connected and used to extract additional information by using reasoning models such as case-based reasoning (CBR) [11].



Taking into account the measures found in the retinal circulation which specify normal values of various retinal structures in healthy subjects, it is possible to apply this information to the study of patients suffering from diseases. Moreover, because of the platform's semi-automated nature and rapid assessment of retinal vessels, it may be helpful in clinical practice.

## 4 Conclusions

Platforms such as Altair, which allow the automated diagnosis of retinal fundal images using digital image analysis, offer a lot of benefits. In a research context, they offer the potential to examine a large number of images with time and cost savings and offer more objective measurements than current observer-driven techniques. Advantages in a clinical context include the potential to perform large numbers of automated screening for conditions such as risk of hypertension, left ventricular hypertrophy, metabolic syndrome, stroke, and coronary artery disease, which in turn reduces the workload required from medical staff. As a future line of study in this point, the next step would be to analyze the significance of the measurements obtained with regard to their meaning in a medical context. That is, to describe the relationship of the results obtained to the risk of cardiovascular disease estimated with the Framingham or similar scale and markers of cardiovascular target organ damage. The platform is intended as a unified tool to link all the methods needed to automate all processes of measurement on the retinas. It uses the latest computer techniques both statistical and medical. Thanks to the experience of the research group at the University of Salamanca ([bisite.usal.es](http://bisite.usal.es)), another line of the future, which is already underway, is the migration of the platform to a cloud environment in which all services are accessible by users, regardless of their location, both safely and ubiquitously [5].

## References

1. Akita, K., Kuga, H.: A computer method of understanding ocular fundus images. *Pattern Recogn.* 16, 431–443 (1982)
2. Chen, B., Toshi, C., Gorin, M.B., Nusinowitz, S.: Analysis of Autofluorescent retinal images and measurement of atrophic lesion growth in Stargardt disease. *Experimental Eye Research* 91(2), 143–152 (2010)
3. Goldbaum, M., Katz, N., Nelson, M., Haff, L.: The discrimination of similarly colored objects in computer images of the ocular fundus. *Invest. Ophthalmol. Vis. Sci.* 31, 617–623 (1990)
4. Heneghan, C., Flynn, J., O'Keefe, M., Cahill, M.: Characterization of changes in blood vessel and tortuosity in retinopathy of prematurity using image analysis. *Med. Image Anal.* 6, 407–429 (2002)

5. Heras, E., De la Prieta, F., Julian, V., Rodríguez, S., Botti, V., Bajo, J., Corchado, J.M.: Agreement technologies and their use in cloud computing environments. *Progress in Artificial Intelligence* 1(4) (2012)
6. Hoover, A., Goldbaum, M.: Locating the optic nerve in a retinal image using the fuzzy convergence of the blood vessels. *IEEE Trans. Biomed. Eng.* 22, 951–958 (2003)
7. Kalviainen, H., Hirvonen, P., Xu, L., Oja, E.: Probabilistic and non-probabilistic Hough transforms. *Image Vision Comput.* 13, 239–252 (1995)
8. Lee, S., Wang, Y., Lee, E.: A computer algorithm for automated detection and quantification of microaneurysms and haemorrhages in color retinal images. In: *SPIE Conference on Image Perception and Performance*, vol. 3663, pp. 61–71 (1999)
9. Li, H., Chutatape, O.: Automated feature extraction in color retinal images by a model based approach. *IEEE Trans. Biomed. Eng.* 51, 246–254 (2004)
10. Patton, N., Aslam, T.M., MacGillivray, T., Deary, I.J., Dhillon, B., Eikelboom, R.H., Yorgesan, K., Constable, I.J.: Retinal image analysis: Concepts, applications and potential. *Progress in Retinal and Eye Research* 25(1), 99–127 (2006)
11. Rodríguez, S., De Paz, J.F., Bajo, J., Corchado, J.M.: Applying CBR Systems to Micro-Array Data Classification. In: Corchado, J.M., De Paz, J.F., Rocha, M.P., Riverola, F.F. (eds.) *Proceedings of IWPAACBB 2008*. ASC, pp. 102–111. Springer, Heidelberg (2010)
12. Sánchez, C., Hornero, R., López, M.I., Aboy, M., Poza, J., Abásolo, D.: A novel automatic image processing algorithm for detection of hard exudates based on retinal image analysis. *Medical Engineering and Physics* 30(1-3), 350–357 (2008)
13. Tamura, S., Okamoto, Y., Yanashima, K.: Zero-crossing interval correction in tracing eye-fundus blood vessels. *Pattern Recogn.* 21, 227–233 (1988)
14. Tanabe, Y., Kawasaki, R., Wang, J.J., Wong, T.Y., Mitchell, P., Daimon, M., et al.: Retinal arteriolar narrowing predicts 5-year risk of hypertension in Japanese people: the Funagata study. *Microcirculation* 17, 94–102 (2010)
15. Wong, T.Y., Duncan, B.B., Golden, S.H., Klein, R., Couper, D.J., Klein, B.E., et al.: Associations between the metabolic syndrome and retinal microvascular signs: the Atherosclerosis Risk In Communities study. *Invest Ophthalmol. Vis. Sci.* 45, 2949–2954 (2004)